






Self-Triggered Based Coordinate Control With Low Communication for Tethered Multi-UAV Collaborative Transportation

Xiaozhen Zhang , Fan Zhang , *Member, IEEE*, Panfeng Huang , *Senior Member, IEEE*, Jiale Gao, Hang Yu , Chongxu Pei, and Yizhai Zhang , *Member, IEEE*

Abstract—In this letter, a self-triggered based coordinate control scheme with low communication requirements is investigated for a team of unmanned aerial vehicles (UAVs) collaboratively transporting a suspended payload. In most existing research on collaborative transportation, the limited communication ability of physical devices has rarely been studied. Hence, this letter suggests a self-triggered cooperative path-following coordinate control scheme for UAVs traveling along a given desired path and synchronously carrying out transportation mission. It is proven that the proposed coordinate control scheme can make communication discrete, thereby significantly reducing the amount of communication. The results of outdoor experiments verify the feasibility of the proposed strategy, and low-frequency communication is demonstrated.

Index Terms—Aerial systems; applications, multi-robot systems, field robots, intelligent transportation systems.

I. INTRODUCTION

A. Motivation

UNMANNED aerial vehicles (UAVs) have played an active role in various aerial cooperative tasks, such as cooperative search [1], surveillance [2], fixed wing recovery [3]–[4] and forest firefighting [5]. Collaborative transportation [6]–[12] has also attracted the interest of many researchers. A team of UAVs can enlarge the load capacity and manipulate a heavier payload

Manuscript received October 10, 2020; accepted January 21, 2021. Date of publication February 4, 2021; date of current version March 2, 2021. This letter was recommended for publication by Associate Editor M. Garratt and Editor P. Pounds upon evaluation of the reviewers' comments. This work was supported in part by National Key R&D Program of China under Grant 2019YFB1310400, in part by the National Natural Science Foundation of China under Grants 61803313, 91848205, 61725303, in part by the Fundamental Research Funds for the Central Universities under Grant 3102019HTQD003, in part by the Young Talent Fund of University Association for Science and Technology in Shaanxi, China under Grant 20190102, in part by the Natural Science Basic Research Plan in Shaanxi Province of China (2019JQ-345, 2019JQ-411, 2019JM-406, 2019JM-392) and in part by the Seed Foundation of Innovation and Creation for Graduate Students in Northwestern Polytechnical University. (*Corresponding author: Fan Zhang.*)

The authors are with the National Key Laboratory of Aerospace Flight Dynamics, Research Center for Intelligent Robotics, School of Astronautics, Northwestern Polytechnical University, Xi'an 710072, China (e-mail: jiaozhen@mail.nwpu.edu.cn; fzhang@nwpu.edu.cn; pffhuang@nwpu.edu.cn; jlgao@mail.nwpu.edu.cn; yuhang@mail.nwpu.edu.cn; peichongxu@mail.nwpu.edu.cn; zhangyizhai@nwpu.edu.cn).

This article has supplementary downloadable material available at <https://doi.org/10.1109/LRA.2021.3057294>, provided by the authors.

Digital Object Identifier 10.1109/LRA.2021.3057294

than can be handled by an individual UAV. The swinging of the payload during acceleration can also be prevented, if more than three UAVs lift the same payload [6].

The communication bandwidth is an important factor in collaborative work. An algorithm with low bandwidth can reduce the requirements of physical communication devices, which is of great significance to practical engineering applications. The motivation of this paper is to investigate a coordinate control scheme with low communication requirements for multi-UAV collaborative transportation.

B. Related Work

A team of UAVs collaboratively transporting a suspended payload is a complex system. Lee in [6]–[7] analyzed the dynamics of multiple UAVs tethering a payload, and demonstrated the high coupling of the motion of the UAVs and the payload. This high coupling complicates the controller design of the system [6]–[8].

For outdoor environments, due to the difficulty of obtaining information about the payload, some researchers [9]–[12] have simplified collaborative transportation by treating the tension caused by the payload as external disturbance to UAVs; Klausen in [10] analyzed the tension disturbance characteristics. In a constant stable transportation case, the tension disturbance can be considered a constant bias, and minor disturbance changes occur when the system acceleration changes.

Cooperative path following (CPF) control [13]–[15] can synchronize the path parameterization variables of each vehicle, and the vehicles follow the path synchronously. Klausen [12] applied CPF control to collaborative transportation without considering communication limitations. However, a low communication approach is more adaptable to outdoor applications.

It is possible to achieve discrete communication by distributed event/self-triggered control [16]. Event/self-triggered control can discretize the control input. If continuous communication must be avoided, two conditions should be followed: 1) the calculation of the triggering law must not require continuous information from neighbor UAVs, and 2) the triggering law should exclude Zeno behavior [17], which is also a key challenge to the design of triggering laws. There have been some triggering laws [18]–[23] proposed, which can exclude Zeno behavior and reduce the communication, but these triggering laws require some

modifications for CPF. Both the author of [19] and [21], considered a leader-following strategy for an event-triggered bipartite consensus, but leader-following strategy is not necessary for CPF. The author in [20] considered measurement noise in event-triggered bipartite consensus. However, the selection of parameters of triggering law is limited and complex in [20] and [21].

Meanwhile, some researchers have successfully applied event/self-triggered control to CPF [24]–[25]. Inspired by the work by Fan [22], Jain in [24] addressed a hybrid self-triggered CPF control scheme for the UAV formation problem, but the calculation of triggering time is aggressive for actual application. Due to the estimation method used, the triggering interval may be very large. The perfection of the physical communication device is required to support the achievement of consensus. Therefore, from an engineering perspective, the method in [24] may not suitable for practical application. Jain in [25] proposed an event-based CPF for the formation of a team of autonomous surface vehicles (AUVs), which aims to reduce communication, but the Zeno behavior was not analyzed.

C. Contribution

The main contribution of this paper is the presentation of a distributed coordinate control scheme for multi-UAV collaborative transportation that has low communication requirements, as well as the experimental verification of the proposed strategy in an outdoor environment. In this work, low-frequency communication is the prime consideration. The tension caused by the payload is treated as disturbance to the UAVs. A self-triggered CPF control scheme is developed for UAVs synchronously traveling along a given desired path. The proposed self-triggered control is proven to exclude Zeno behavior, which guarantees discrete low-frequency communication between UAVs. Compared with [12], the communication frequency can be significantly reduced. Compared with [24], the proposed algorithm is conservative for safe application and verified by experiments. Moreover, compared with [25], proposed algorithm is proven the Zeno behavior will not happen, which theoretically guarantees the discontinuity of communication.

The remainder of this paper is organized as follows. The detailed problem is described in Section II. Then, in Section III, a self-triggered coordinate control scheme with low communication requirements is addressed, and its stability is analyzed. The proposed self-triggered coordinate control scheme is proven without Zeno behavior. Further, in Section IV, a simulation is done to verify proposed self-triggered coordinate control and compare with the continuous approach. Finally, the detailed configuration of the experimental system, the scenario of the transportation mission, and the experimental results are reported in Section V.

II. PRELIMINARIES AND PROBLEM STATEMENT

A. Graph Theory

A directed graph \mathcal{G} is a pair $(\mathcal{V}, \mathcal{E})$, where $\mathcal{V} = \{v_1, \dots, v_N\}$ is a non-empty finite set of nodes and $\mathcal{E} \subseteq \mathcal{V} \times \mathcal{V}$ is a set of ordered pairs of nodes, called edges. An edge (v_j, v_i) represents



Fig. 1. Three tethered UAVs collaboratively transporting a payload.

the communication path from node v_j to node v_i meaning the node v_j is one of the neighbors of node v_i , and is defined as

$$\begin{aligned} a_{ij} &> 0 \Leftrightarrow (v_j, v_i) \in \mathcal{E}, \\ a_{ij} &= 0 \Leftrightarrow (v_j, v_i) \notin \mathcal{E}, \end{aligned}$$

where $\mathcal{A} = [a_{ij}] \in \mathbb{R}^{N \times N}$ is the adjacency matrix of graph \mathcal{G} . In general, $a_{ii} = 0$ is defined. The set $\mathcal{N}_i = \{j \in \mathcal{V} : (v_j, v_i) \in \mathcal{E}\}$ contains all neighbors of node v_i .

The degree matrix \mathcal{D} of graph \mathcal{G} is defined as

$$\begin{aligned} \mathcal{D} &= \text{diag}(d_1, d_2, \dots, d_n), \\ d_i &= \sum_{j=1}^n a_{ij} = \sum_{j \in \mathcal{N}_i} a_{ij}. \end{aligned}$$

The Laplacian matrix $\mathcal{L} = [l_{ij}] \in \mathbb{R}^{N \times N}$ is defined as:

$$\mathcal{L} = \mathcal{D} - \mathcal{A} = \begin{bmatrix} \sum_{j \in \mathcal{N}_1} a_{1j} & -a_{12} & \cdots & -a_{1n} \\ -a_{21} & \sum_{j \in \mathcal{N}_2} a_{2j} & \cdots & -a_{2n} \\ \vdots & \vdots & \ddots & \vdots \\ -a_{n1} & -a_{n2} & \cdots & \sum_{j \in \mathcal{N}_n} a_{nj} \end{bmatrix}.$$

Lemma 1 ([26]): If a graph is connected, then its Laplacian matrix \mathcal{L} is positive semidefinite. The following inequality holds:

$$0 \leq \rho_2(\mathcal{L}) \left(\mathbf{I}_n - \frac{1}{n} \mathbf{1}_n \mathbf{1}_n^T \right) \leq \mathcal{L},$$

where $\rho_2(\mathcal{L})$ indicates the minimum positive eigenvalue for \mathcal{L} .

B. Problem Description

As shown in Fig. 1, consider n ($n \geq 3$) UAVs collaboratively transporting a payload. A mission path $\mathbf{p}_{mission}^d(\gamma) \in \mathbb{R}^3$ and transportation formation $\mathbf{r}_i^d(\gamma) \in \mathbb{R}^3$ are given for the team of UAVs.

The desired path $\mathbf{p}_i^d(\gamma)$ of each UAV is

$$\mathbf{p}_i^d(\gamma) = \mathbf{p}_{mission}^d(\gamma) + \mathbf{r}_i^d(\gamma). \quad (1)$$

Because there is no coordinator in the system, each UAV may start the mission at different times t_{start}^i . Two types of important times in a transportation mission are subsequently defined.

Definition 1 (Absolute Mission Time): The absolute mission time t is the same as the usual time in the real world. The assessment of the transportation experimental results is conducted in absolute mission time.

Definition 2 (Local Mission Time): The local mission time $\gamma_i(t)$ refers to the path-following times of different UAVs. $\gamma_i(0) = 0$, and $\gamma_i(t)$ is defined as

$$\dot{\gamma}_i(t) = \begin{cases} 0 & t \leq t_{start}^i \\ \mu_i(t) + v_d & t > t_{start}^i \end{cases} \quad (2)$$

where $v_d = 1$ and $\mu_i(t)$ is an extra input used to synchronize the local mission time $\gamma_i(t)$ with those of other UAVs.

Remark 1: In general, in CPF (e.g., [12], [24]–[25]), the path parameter $\gamma_i(t)$ is in charge of a speed v_d , as shown in (2). Because $\mathbf{p}_{mission}^d(\gamma)$ is usually designed by $\mathbf{p}_{mission}^d(t)$, a local mission time is defined by setting $v_d = \dot{t} = 1$. A similar setting was used in the research by [14].

In this paper, the tension caused by the payload is treated as external disturbance to the UAVs, which can be rejected by individual UAV position control. The synchronization and coordination of UAVs should be considered as a consensus problem. Hence, the collaborative transportation problem is separated into two sub-problems, as following.

Problem 1 (Path-Following Problem): Each UAV tracks the desired path $\mathbf{p}_i^d(\gamma_i(t))$ in the presence of tension and wind disturbance.

Problem 2 (Local Mission Time Coordination Problem): The UAVs follow their desired path synchronously, which means the consensus of the local mission time, $|\gamma_i(t) - \gamma_j(t)| \rightarrow 0$.

Problem 1 is a classical position tracking problem under an unknown tension and wind disturbance of a UAV. This topic has been widely studied [28]–[29]. For Problem 2, this paper suggests a self-triggered coordinate control with low communication requirement.

III. SELF-TRIGGERED COORDINATE CONTROL DESIGN

This section focuses on Problem 2 defined in Sec II. The desired path $\mathbf{p}_i^d(\gamma_i(t))$ is only known to the i -th UAV, which starts the mission at absolute mission time t_{start}^i , that $\gamma(t_{start}^i) = 0$.

If each UAV shares a coincident local mission time, that $\gamma_i(t) = \gamma_j(t)$, the UAVs will travel along the given desired path $\mathbf{p}_i^d(\gamma_i(t))$ synchronously.

A classical consensus protocol ([27]) for system (2) is given as follows:

$$\mu(t) = -k_c \mathcal{L} \gamma(t). \quad (3)$$

It is evident that (3) requires continuous state information from the neighbor UAVs, but the communication ability of the physical device is always limited. Thus, a discrete protocol can be a superior choice. If the i -th UAV only broadcasts its state information at its triggering time $\{t_k^i\}_{k=1}^\infty$, the discrete

consensus protocol is

$$\mu_i(t) = -k \sum_{j=1}^n l_{ij} \widehat{\gamma}_j(t), \quad (4)$$

where $k > 0$ and

$$\widehat{\gamma}_j(t) = \gamma_j(t_k^j) + 1 \left(t - t_k^j \right) t \in \left[t_k^j, t_{k+1}^j \right).$$

When i -th UAV starts the mission, the first triggering time is determined to be $t_1^i = t_{start}^i$. Here consider a self-triggered way to determine the triggering time sequence $\{t_k^i\}_{k=2}^\infty$:

$$t_{k+1}^i = \max_{r \geq t_k^i} \left\{ r : |e_i(t)| \leq \frac{\alpha}{\sqrt{l_{ii}}} e^{-\beta t} \forall t \in [t_k^i, r) \right\}, \quad (5)$$

where $e_i(t) = \widehat{\gamma}_i(t) - \gamma_i(t)$, $\alpha > 0$ and $\beta > 0$.

Theorem 1: Under an undirected graph \mathcal{G} , consider the system (2), the local mission time $\gamma_i(t)$ of the UAVs will achieve consensus by the self-triggered control (4) with the triggering time determined by (5), and no Zeno behavior will happen.

Proof: i). First study the consensus of $\gamma_i(t)$.

Consider the average:

$$\bar{\gamma}(t) = \frac{1}{n} \sum_{i=1}^n \gamma_i(t). \quad (6)$$

The derivative of $\bar{\gamma}(t)$ is

$$\begin{aligned} \dot{\bar{\gamma}}(t) &= \frac{1}{n} \sum_{i=1}^n \dot{\gamma}_i(t) = 1 + \frac{k}{n} \sum_{i=1}^n \sum_{j=1}^n l_{ij} \widehat{\gamma}_j(t) \\ &= 1 + \frac{k}{n} \sum_{i=1}^n \sum_{j=1}^n l_{ij} e_i(t) + \frac{k}{n} \sum_{i=1}^n \sum_{j=1}^n l_{ij} \gamma_j(t) = 1. \end{aligned} \quad (7)$$

Define

$$\delta_i(t) = \gamma_i(t) - \bar{\gamma}(t). \quad (8)$$

Consider such a Lyapunov function:

$$\begin{aligned} V(\gamma(t)) &= \frac{1}{2} \gamma^T \left(\mathbf{I}_n - \frac{1}{n} \mathbf{1} \mathbf{1}^T \right) \gamma \\ &= \frac{1}{2} \sum_{i=1}^n (\gamma_i(t) - \bar{\gamma}(t))^2 \\ &= \frac{1}{2} \sum_{i=1}^n \delta_i^2(t). \end{aligned} \quad (9)$$

The derivative of $V(\gamma(t))$ along system (2) is

$$\begin{aligned} \dot{V}(\gamma(t)) &= \sum_{i=1}^n (\gamma_i(t) - \bar{\gamma}(t)) (\dot{\gamma}_i(t) - \dot{\bar{\gamma}}(t)) \\ &= \sum_{i=1}^n (\gamma_i(t) - \bar{\gamma}(t)) \left(-k \sum_{j=1}^n l_{ij} \widehat{\gamma}_j(t) + 1 - 1 \right) \\ &= -k \sum_{i=1}^n \gamma_i(t) \sum_{j=1}^n l_{ij} \widehat{\gamma}_j(t). \end{aligned}$$

Consider the consensus:

$$\begin{aligned} \sum_{i=1}^n q_i(t) &= -\sum_{i=1}^n \frac{1}{2} \sum_{j \in \mathcal{N}_i} l_{ij} (\gamma_i(t) - \gamma_j(t))^2 \\ &= \gamma^T(t) \mathcal{L} \gamma(t). \end{aligned} \quad (10)$$

Then,

$$\begin{aligned} \dot{V}(\gamma(t)) &= -k \sum_{i=1}^n \gamma_i(t) \sum_{j=1}^n l_{ij} \widehat{\gamma}_j(t) \\ &= -k \sum_{i=1}^n \gamma_i(t) \sum_{j=1}^n l_{ij} (\gamma_j(t) + e_j(t)) \\ &= -k \sum_{i=1}^n q_i(t) - k \sum_{i=1}^n e_i(t) \sum_{j=1}^n l_{ij} \gamma_j(t) \\ &\leq -\frac{k}{2} \sum_{i=1}^n q_i(t) + k \sum_{i=1}^n l_{ii} e_i^2(t). \end{aligned}$$

According to (5) and Lemma 1, we have

$$\begin{aligned} \dot{V}(\gamma(t)) &= -\frac{k}{2} \gamma^T(t) \mathcal{L} \gamma(t) + k \sum_{i=1}^n l_{ii} e_i^2(t) \\ &\leq -\frac{k}{2} \rho_2(\mathcal{L}) V(\gamma(t)) + nk\alpha^2 e^{-\beta t} \\ &\leq -\kappa V(\gamma(t)) + C, \end{aligned} \quad (11)$$

where $\kappa = \frac{k}{2} \rho_2(\mathcal{L}) > 0$ and $C = nk\alpha^2 > 0$.

This implies that system (2) will reach consensus under the discrete protocol (4) with the triggering time sequence determined by (5).

Remark 2: (11) implies $\gamma_i(t)$ will converge to the neighborhood of $\bar{\gamma}(t)$, and the size of the neighborhood is related to $nk\alpha^2 e^{-\beta t}$. k and the parameters α and β of triggering law (5) can impact the performance of proposed self-triggered control (4). On the other hand, the continuous protocol (3) will converge to $\bar{\gamma}(t)$, which implies the continuous protocol will certainly have a better performance than self-triggered control. Hence, as a cost of convergence performance, communication requirement can be reduced under proposed self-triggered control. For users, the parameters should be adjusted according to the allowable convergence neighborhood. A trade-off between communication reduction and convergence performance should be considered.

ii). Next, Zeno behavior will be analyzed. The lower bound of triggering intervals will be proved to be a positive constant.

Solve (11), we have

$$V(\gamma(t)) \leq c_1 e^{-\kappa t} + c_2 e^{-\beta t}, \quad (12)$$

where,

$$c_1 = \begin{cases} V(\gamma(0)) - \frac{n\alpha^2}{\kappa - \beta} & \kappa \neq \beta \\ V(\gamma(0)) & \kappa = \beta \end{cases},$$

$$c_2 = \begin{cases} \frac{n\alpha^2}{\kappa - \beta} & \kappa \neq \beta \\ n\alpha^2 t & \kappa = \beta \end{cases}.$$

Notice

$$\begin{aligned} \gamma_i(t) - \gamma_j(t) &= (\gamma_i(t) - \bar{\gamma}(t)) - (\gamma_j(t) - \bar{\gamma}(t)) \\ &= \delta_i(t) - \delta_j(t). \end{aligned}$$

Now estimate the upper bound of $|\mu_i(t)|$,

$$\begin{aligned} |\mu_i(t)| &= \left| k \sum_{j \in \mathcal{N}_i} \widehat{\gamma}_j(t) \right| = \left| k \sum_{j \in \mathcal{N}_i} (\delta_j(t) - e_j(t)) \right| \\ &\leq \left| k \sum_{j \in \mathcal{N}_i} \delta_j(t) \right| + \left| k \sum_{j \in \mathcal{N}_i} e_j(t) \right|. \end{aligned}$$

According to (12), there exist a finite constant $M = \sup_{t>0} (V(\gamma(t)))$.

Consider

$$\left| k \sum_{j \in \mathcal{N}_i} \delta_j(t) \right| \leq \left| k \sum_{j=1}^n \delta_j(t) \right| \leq \sqrt{\frac{k \sum_{i=1}^n \delta_i^2(t)}{n}} \leq \sqrt{\frac{2kM}{n}}.$$

According to (5), we have

$$\left| k \sum_{j \in \mathcal{N}_i} e_j(t) \right| \leq k\alpha \sqrt{l_{ii}} e^{-\frac{\beta}{2}t} \leq k\alpha \sqrt{l_{ii}}.$$

Thus,

$$\begin{aligned} |\mu_i(t)| &\leq \left| k \sum_{j \in \mathcal{N}_i} \delta_j(t) \right| + \left| k \sum_{j \in \mathcal{N}_i} e_j(t) \right| \\ &\leq \sqrt{\frac{2kM}{n}} + k\alpha \sqrt{l_{ii}} = \mu_{\text{sup}}. \end{aligned}$$

Consider any triggering time of i th-UAV $t_k^i > 0$. The lower bound of the error $|e_i(t)|$ is

$$\begin{aligned} |e_i(t)| &= |\widehat{\gamma}_i(t) - \gamma_i(t)| \\ &= \left| -\int_{t_k^i}^t \mu_i(t) dt \right| \leq (t - t_k^i) \mu_{\text{sup}}. \end{aligned} \quad (13)$$

According to (5) and (13), Consider any triggering interval $\tau = (t - t_k^i)$,

$$\tau \geq \frac{|e_i(t)|}{\mu_{\text{sup}}} \geq \frac{\alpha}{\mu_{\text{sup}} \sqrt{l_{ii}}} e^{-\frac{\beta}{2}\tau}. \quad (14)$$

According to the increase and decrease of exponential function and first order function. There exist an unique positive constant solution $\tau_{\text{inf}} > 0$ for (14). This solution τ_{inf} also is the lower bound of triggering intervals, which means Zeno behavior will not happen.

Remark 3: As shown in Fig. 2. Proposed self-triggered coordinate control is the only component that requires communication. UAVs only send their states to their neighbors at their triggering time sequence determined by (5). Because (5) only depends on i -th UAV's own states, proposed coordinate control scheme is called self-triggered.

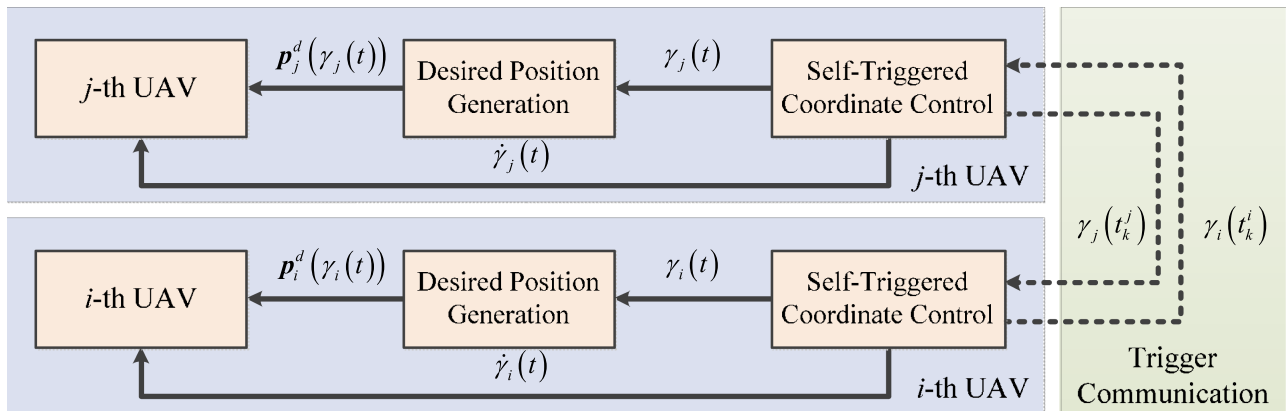


Fig. 2. Communication Data flow of the system.



Fig. 3. Communication topology of the UAVs.

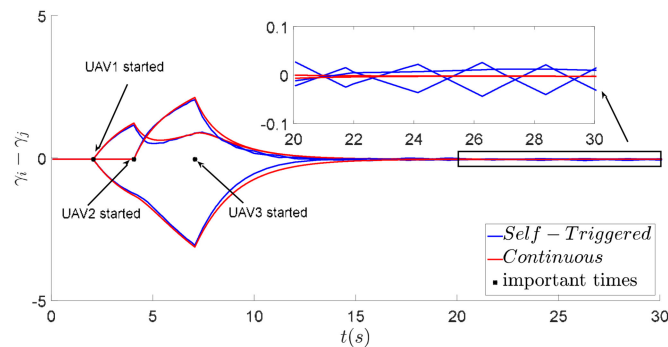


Fig. 4. Comparison between self-triggered and continuous approach.

Remark 4: It is proven that Zeno behavior will not happen. Hence, the triggering time sequence is proven to be discretized. Further, continuous communication is also avoided.

IV. SIMULATION

In this section, a simulation was conducted to verify proposed self-triggered coordinate control in Sec III. For a same consensus problem, the continuous method and the proposed self-triggered method were used.

The parameters of continuous control (3) was $k_c = 0.5$. The parameters of proposed self-triggered control (4) and (5) were selected as $k = 0.5$, $\alpha = 0.5$ and $\beta = 2$.

The communication topology of the three UAVs is presented in Fig. 3.

In simulation, the start time of three UAVs are set as $t_{start}^1 = 2$ s, $t_{start}^2 = 4$ s and $t_{start}^3 = 7$ s. Fig. 4 showed the results of two kinds of method. The convergence process of the two methods was similar, and both can achieve consensus.

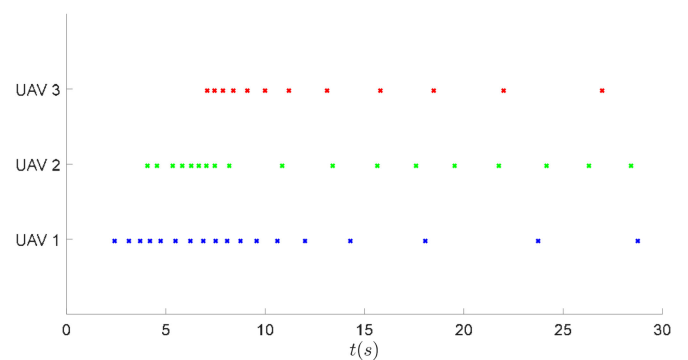


Fig. 5. Triggering times in simulation.

Fig. 4 also presented the details performance of the consensus phase (20 s~30 s). The continuous method was better than self-triggered. The theoretical analysis of causes has been addressed in Remark 2. As shown in Fig. 5, in 30 seconds of simulation, three UAVs only broadcasted their local mission time $\gamma_i(t)$ 18, 18 and 12 times, respectively. The amount of communications was evidently reduced under proposed self-triggered control, and an acceptable consensus was also achieved.

Hence, According to the comparison results, it can be concluded that the proposed self-triggered method can also achieve the similar performance of continuous method. And proposed self-triggered control can effectively reduce the amount of communications.

V. EXPERIMENTAL RESULTS

Experiments were performed to investigate the effectiveness of the approach proposed in Sec III.

The control parameters in Sec III were selected as $k = 0.5$, $\alpha = 0.5$ and $\beta = 2$.

A. Experimental System Description

The utilized UAVs were DJI Matrice 210¹ (M210). M210 is a powerful aerial platform, which equipped with external disturbance rejection ability. DJI Technology Co. provides the Mobile

¹<https://www.dji.com/cn/matrice-200-series>

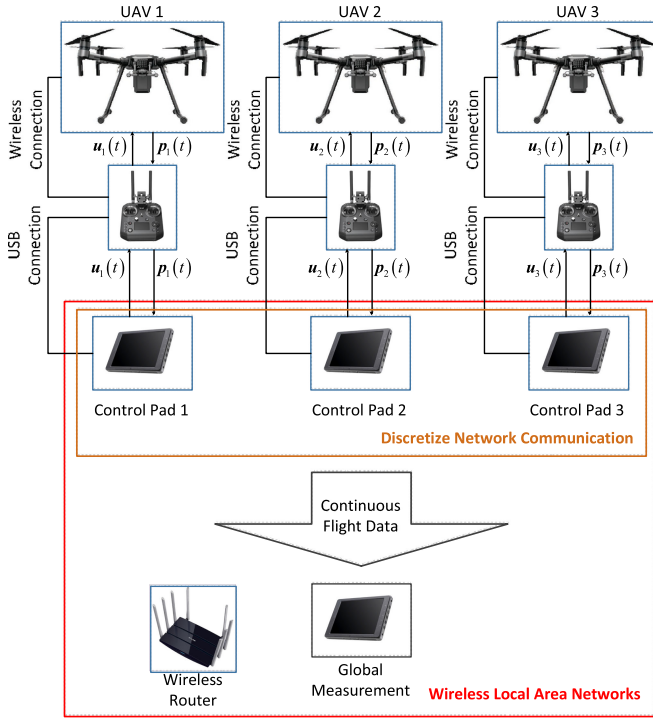


Fig. 6. Experimental system and data flow in physical devices.

SDK² (MSDK) for developers to control the M210. When developers use MSDK, the control input is the desired velocity of M210, and M210 will track the inputted desired velocity under external disturbance. A feedback control is designed for UAV position tracking (Problem 1).

Corresponding to Fig. 2, Fig. 6 presents the information flow of the practical experiment. The control program was installed on Android control Pads. To achieve the consensus of the local mission time $\gamma_i(t)$ (Problem 2), the Pads communicated with each other via wireless local area networks (WLANs). Additionally, by transferring via remote control, each control Pad could obtain the flight data of the UAV and send command to achieve path-following (Problem 1). Besides, there was a Pad utilized for global measurement in absolute mission time. This Pad did not participate in the mission, and only collected control and flight data for the analysis of the results in unified absolute mission time.

B. Transportation Mission Scenario

The transportation mission scenario was three UAVs collaboratively transporting a 1.7kg payload along the mission path with a fixed formation. Different UAVs started the mission at different absolute mission times.

Each UAV was connected to the payload by a cable of length 14m. Due to the length of tethered cable were same, we just gave a regular triangle on the horizontal plane with a side length of

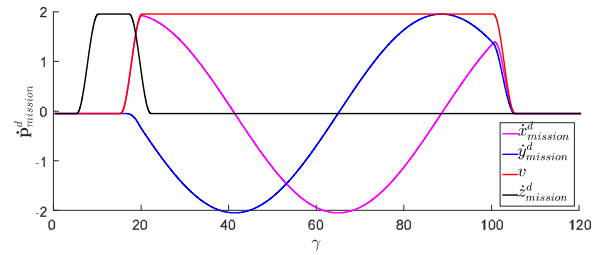


Fig. 7. The derivative of the mission path.

12m formation to UAVs.

$$\begin{cases} r_1^d = [0 \ 6\sqrt{3} \ 0]^T \\ r_2^d = [-6 \ -3\sqrt{3} \ 0]^T \\ r_3^d = [6 \ -3\sqrt{3} \ 0]^T \end{cases}$$

As shown in Fig. 3, the communication topology of UAVs in experiment is same as configuration of simulation in Section IV.

Synchronization is very important in UAVs collaborative transportation. If one UAV had risen ahead of others, accident might occur due to the tethered cable. Hence, for safety reasons, a period of low altitude hovering was consider in transportation mission path $\mathbf{p}_{mission}^d(\gamma)$ design for waiting the reduction of consensus error of local mission time.

The mission path is designed as a continuous smooth and bounded.

$$\dot{\mathbf{p}}_{mission}^d(\gamma) = [\dot{x}_{mission}^d(\gamma) \ \dot{y}_{mission}^d(\gamma) \ \dot{z}_{mission}^d(\gamma)]^T,$$

$$\dot{x}_{mission}^d(\gamma) = v(\gamma) \cos\left(\frac{-\int_0^\gamma v(\tau) d\tau}{30}\right),$$

$$\dot{y}_{mission}^d(\gamma) = v(\gamma) \sin\left(\frac{-\int_0^\gamma v(\tau) d\tau}{30}\right),$$

$$z_{mission}^d(\gamma) = \begin{cases} 0 & \gamma \in [0, 5) \cup [22, +\infty) \\ 1 - \cos\left(\frac{2(\gamma-5)}{\pi}\right) & \gamma \in [5, 10) \\ 2 & \gamma \in [10, 17) \\ 1 + \cos\left(\frac{2(\gamma-17)}{\pi}\right) & \gamma \in [17, 22) \end{cases},$$

$$v(\gamma) = \begin{cases} 0 & \gamma \in [0, 15) \cup [105, +\infty) \\ 1 - \cos\left(\frac{2(\gamma-15)}{\pi}\right) & \gamma \in [15, 20) \\ 2 & \gamma \in [20, 100) \\ 1 + \cos\left(\frac{2(\gamma-100)}{\pi}\right) & \gamma \in [100, 105) \end{cases}.$$

Note that $\dot{x}_{mission}^d(\gamma)$ and $\dot{y}_{mission}^d(\gamma)$ are components of $v(\gamma)$, and the horizontal motion speed of mission path is determined by $v(\gamma)$, holding

$$\sqrt{(\dot{x}_{mission}^d(\gamma))^2 + (\dot{y}_{mission}^d(\gamma))^2} = v(\gamma).$$

The derivative of the mission path is shown in Fig. 7, and the entire path is presented in Fig. 8.

²<https://developer.dji.com/mobile-sdk>

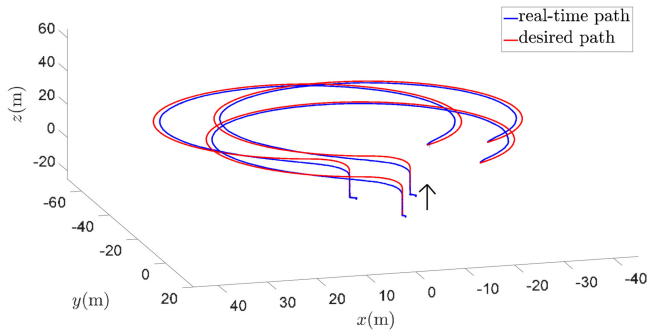


Fig. 8. Path of collaborative transportation.

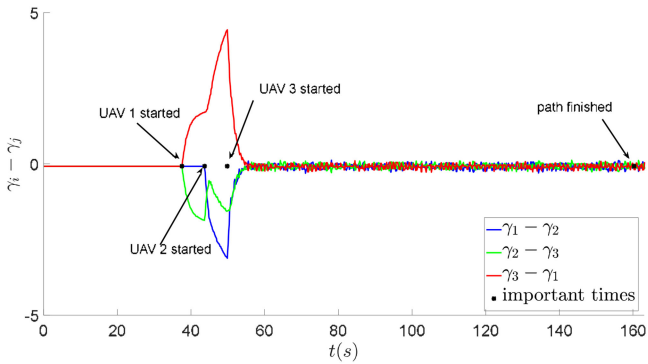


Fig. 9. Consensus of local mission times γ_i .

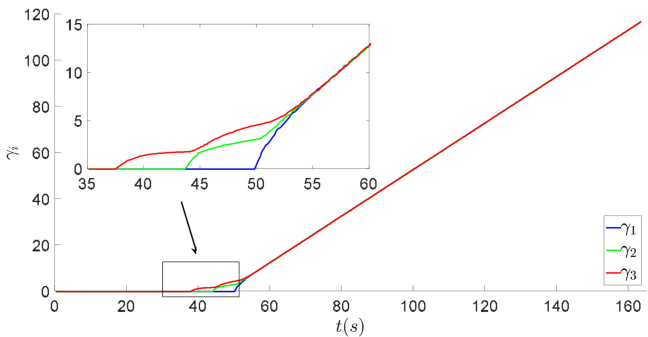


Fig. 10. Local mission times γ_i .

C. Experimental Results Analysis

The experimental results were collected and recorded by the global measurement Pad (shown in Fig. 6) in unified absolute mission time.

As determined from the experimental results, three UAVs respectively started mission at 37.4 s, 43.5 s and 49.7 s, and all UAVs finished the transportation mission path at 160 s.

The overall transportation mission path is presented in Fig. 8. UAVs first rose and then entered a circular transportation path. For most of the transportation mission time, UAVs traveled synchronously. Fig. 13 presented the formation keeping error also remained within a small range during the mission, which was due to the well synchronization of the UAVs, and which also ensured the safety of transportation. The consensus of the local mission times was shown in Fig. 9 and Fig. 10. After all

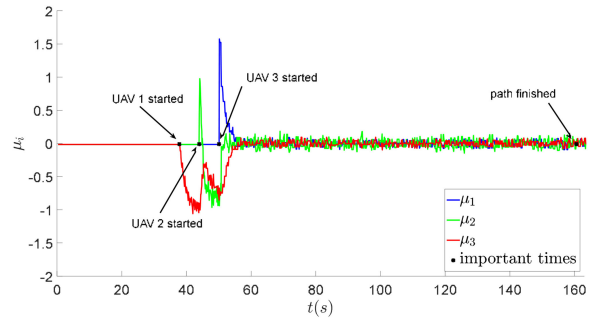


Fig. 11. Input of self-triggered coordinate control μ_i .

TABLE I
COMPARISON OF SELF-TRIGGERED AND CONTINUOUS APPROACHES

	UAV 1	UAV 2	UAV 3
Duration (s)	110.3	116.5	122.6
Periodic	1103	1165	1226
Triggered times	41	54	62
Communication Reduction (%)	96.28	95.36	94.94

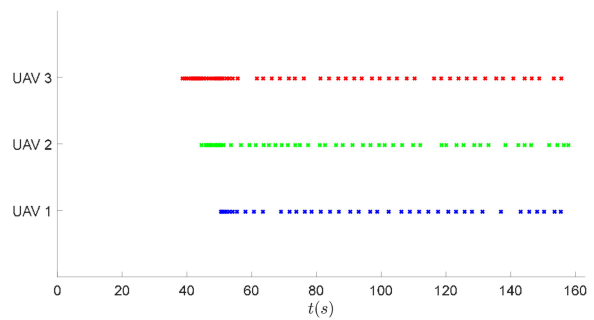


Fig. 12. Triggering times of UAVs.

UAVs started the mission, γ_i soon reached and maintained in consensus. From 37 s to 60 s, as shown in Fig. 10 and Fig. 11, the input μ_i made a significant contribution to the consensus. UAVs adjusted the speed of their local mission time $\dot{\gamma}_i$ by (2). After consensus was achieved, μ_i tended to zero. Compared with the simulation in Section IV, the consensus performance was inferior for the reason of network communication time delay. According to the test, delay of WIFI network is generally around 100 ms. Small WIFI delay has limited impact on consensus. The synchronization of UAVs still held good enough performance, which can be seen in the video. However, from a theoretical point of view, time delay is a problem worth exploring. We will do some work in this theme on the future.

The running period of the control program in the Android Pads was 0.1s and the coordinate control (4)–(5) period was also 0.1s. For continuous approach, each Android Pad will broadcast its local mission time γ_i every control period. As exhibited in Table I, the UAV durations of mission are 110.3 s, 116.5 s and 122.6 s, respectively. Therefore, theoretically, the amount of data broadcast required by the continuous approach is more than 1000 times. However, Fig. 12 presented the proposed discrete communication in experiment. Three UAVs broadcasted data

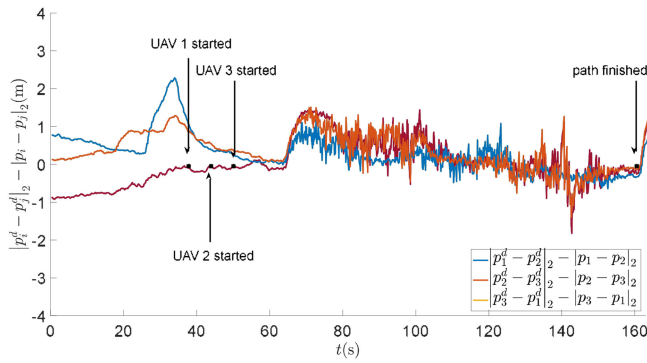


Fig. 13. Formation keeping error.

only 41, 54 and 62 times, respectively. Compared with the continuous approach, the communication requirement was reduced by more than 94% via the proposed discrete self-triggered algorithm.

VI. CONCLUSION

In this work, a self-triggered cooperative path-following coordinate control scheme for collaborative transportation by a team of tethered UAVs was developed. The proposed method can discretize the communication between UAVs, which greatly reduces the burden on physical communication devices. An outdoor experiment was conducted to validate the effectiveness of the proposed method, and the results demonstrated that the UAVs could collaborative transport a payload along the given mission path synchronously. Additionally, the communication requirement was found to be reduced by more than 94% as compared with the continuous approach.

The time delay and pocket lost problem in self-triggered CPF may be studied in future work. It would also be interesting to investigate a control approach with low communication requirements without a pre-defined mission path.

REFERENCES

- [1] A. Wallar, E. Plaku, and D. A. Sofge, "Reactive motion planning for unmanned aerial surveillance of risk-sensitive areas," *IEEE T. Autom. Sci. Eng.*, vol. 12, no. 3, pp. 969–980, Jul. 2015.
- [2] J. Gu, T. Su, Q. Wang, X. Du, and M. Guizani, "Multiple moving targets surveillance based on a cooperative network for Multi-UAV," *IEEE Commun. Mag.*, vol. 56, no. 4, pp. 82–89, Apr. 2018.
- [3] R. Skulstad, C. Syversen, M. Merz, N. Sokolova, T. Fossen, and T. Johansen, "Autonomous net recovery of fixed-wing UAV with single-frequency carrier-phase differential GNSS," *IEEE Aero. El. Sys. Mag.*, vol. 30, no. 5, pp. 18–27, May 2015.
- [4] K. Klausen, T. I. Fossen, and T. A. Johansen, "Autonomous recovery of a fixed-wing UAV using a net suspended by two multirotor UAVs," *J. Field Robot.*, vol. 35, no. 5, pp. 717–731, 2018.
- [5] K. Harikumar, J. Senthilnath, and S. Sundaram, "Multi-UAV oxyrrhis marina-inspired search and dynamic formation control for forest firefighting," *IEEE T. Autom. Sci. Eng.*, vol. 16, no. 2, pp. 863–873, Apr. 2019.
- [6] T. Lee, K. Sreenath, and V. Kumar, "Geometric control of cooperating multiple quadrotor UAVs with a suspended payload," in *Proc. 52nd IEEE Conf. Decis. Control*, Dec. 2013, pp. 5510–5515.
- [7] T. Lee, "Geometric control of quadrotor UAVs transporting a cable-suspended rigid body," *IEEE T. Contr. Syst. T.*, vol. 26, no. 1, pp. 255–264, Jan. 2018.
- [8] B. Shirani, M. Najafi, and I. Izadi, "Cooperative load transportation using multiple UAVs," *Aerosp. Sci. Technol.*, vol. 84, pp. 158–169, Jan. 2019.
- [9] H. G. d. Marina and E. Smeur, "Flexible collaborative transportation by a team of rotorcraft," in *Proc. Int. Conf. Robot. Autom.*, May 2019, pp. 1074–1080.
- [10] K. Klausen, C. Meissen, T. I. Fossen, M. Arcak, and T. A. Johansen, "Cooperative control for multirotors transporting an unknown suspended load under environmental disturbances," *IEEE T. Contr. Syst. T.*, vol. 28, no. 2, pp. 653–660, Mar. 2020.
- [11] I. H. B. Pizetta, A. S. Brandão, and M. Sarcinelli-Filho, "Cooperative load transportation using three quadrotors," in *Proc. 2019 Int. Conf. Unmanned Aircr. Syst.*, Jun. 2017, pp. 644–650.
- [12] K. Klausen, T. I. Fossen, T. A. Johansen, and A. P. Aguiar, "Cooperative path-following for multirotor UAVs with a suspended payload," in *Proc. IEEE Conf. Control Appl.*, Sep. 2015, pp. 1354–1360.
- [13] R. Ghabelchloo, A. P. Aguiar, A. Pascoal, C. Silvestre, I. Kaminer, and J. Hespanha, "Coordinated path-following in the presence of communication losses and time delays," *SIAM J. Control Optim.*, vol. 48, no. 1, pp. 234–265, 2009.
- [14] V. Cichella *et al.*, "Cooperative path following of multiple multirotors over time-varying networks," *IEEE T. Autom. Sci. Eng.*, vol. 12, no. 3, pp. 945–957, Jul. 2015.
- [15] E. Xargay *et al.*, "Time-critical cooperative path following of multiple UAVs over time-varying networks," *J. Guid., Control Dyn.*, vol. 36, no. 2, pp. 499–516, Mar.–Apr. 2013.
- [16] L. Ding, Q. Han, X. Ge, and X. Zhang, "An overview of recent advances in event-triggered consensus of multiagent systems," *IEEE T. Cybern.*, vol. 48, no. 4, pp. 1110–1123, Apr. 2018.
- [17] K. H. Johansson, M. Egerstedt, J. Lygeros, and S. Sastry, "On the regularization of zero hybrid automata," *Syst. Control Lett.*, vol. 38, no. 3, pp. 141–150, 1999.
- [18] G. S. Seyboth, D. V. Dimarogonas, and K. H. Johansson, "Event-based broadcasting for multi-agent average consensus," *Automatica*, vol. 49, no. 1, pp. 245–252, Jan. 2013.
- [19] J. Ren, Q. Song, and G. Lu, "Event-triggered bipartite leader-following consensus of second-order nonlinear multi-agent systems under signed digraph," *J. Franklin I.*, vol. 356, no. 12, pp. 6591–6609, Aug. 2019.
- [20] C. Ma, Y. Zhao, and W. Sun, "Event-Triggered bipartite consensus of single-integrator multi-agent systems with measurement noise," *J. Control Sci. Eng.*, vol. 2018, pp. 1–9, 2018.
- [21] A. Hu, Y. Wang, J. Cao, and A. Alsaedi, "Event-triggered bipartite consensus of multi-agent systems with switching partial couplings and topologies," *Inform. Sci.*, vol. 521, pp. 1–13, Jun. 2020.
- [22] Y. Fan, L. Liu, G. Feng, and Y. Wang, "Self-Triggered consensus for multi-agent systems with zero-free triggers," *IEEE T. Automat. Contr.*, vol. 60, no. 10, pp. 2779–2784, Oct. 2015.
- [23] X. Yi, K. Liu, D. V. Dimarogonas, and K. H. Johansson, "Dynamic event-triggered and self-triggered control for Multi-agent systems," *IEEE T. Automat. Contr.*, vol. 64, no. 8, pp. 3300–3307, Aug. 2019.
- [24] R. P. Jain, A. P. Aguiar, and J. Sousa, "Self-triggered cooperative path following control of fixed wing unmanned aerial vehicles," in *Proc. Int. Conf. Unmanned Aircr. Syst.*, Jun. 2017, pp. 1231–1240.
- [25] R. P. Jain, A. P. Aguiar, and J. B. de Sousa, "Cooperative path following of robotic vehicles using an event-based control and communication strategy," *IEEE Robot. Automat. Lett.*, vol. 3, no. 3, pp. 1941–1948, Jul. 2018.
- [26] M. Mesbahi and M. Egerstedt, *Graph Theoretic Methods in Multi-Agent Networks*. Princeton, NJ, USA: Princeton Univ. Press, 2010.
- [27] R. Olfati-Saber, J. A. Fax, and R. M. Murray, "Consensus and cooperation in networked multi-agent systems," *Proc. IEEE*, vol. 95, no. 1, pp. 215–233, Jan. 2007.
- [28] S. Islam, P. X. Liu, and A. E. Saddik, "Robust control of four-rotor unmanned aerial vehicle with disturbance uncertainty," *IEEE T. Ind. Electron.*, vol. 62, no. 3, pp. 1563–1571, Mar. 2015.
- [29] L. Wang and J. Su, "Robust disturbance rejection control for attitude tracking of an aircraft," *IEEE T. Contr. Syst. T.*, vol. 23, no. 6, pp. 2361–2368, Nov. 2015.